

UC Davis
IDAV Publications

Title

Visualization of Seismic Soil Structure Interaction Simulations

Permalink

<https://escholarship.org/uc/item/4x30r2vp>

Authors

Scheuermann, Gerik
Frey, Jan
Hagen, Hans
et al.

Publication Date

2001

Peer reviewed

Visualization of Seismic Soils Structure Interaction Simulations

GERIK SCHEUERMANN^{1,2}, JAN FREY¹, HANS HAGEN¹, BERND HAMANN², BORIS JEREMIC³,
KENNETH I. JOY²

¹ Computer Science Department, University of Kaiserslautern, P.O. Box 3049,
D-67653 Kaiserslautern, Germany

² Center of Image Processing and Integrated Computing, Department of Computer Science,
University of California, 1 Shields Avenue, Davis, CA 95616-8562, USA

³ Center for Geotechnical Modeling, Civil and Environmental Engineering Department,
University of California, 1 Shields Avenue, Davis, CA 95616, USA

Abstract

Earthquake events are among the most devastating catastrophes on Earth. Besides human casualties, they are also responsible for large damage to a variety of man-built objects. Civil engineering thus has significant interest in understanding effects of earthquakes. Induced dynamic motions will cause significant oscillations in stress and strain tensors inside 3D solids (soils, concrete and steel). These fluctuations in stresses and strains can result in failure of one of the components of the civil engineering object which might eventually lead to the complete failure and loss of life. We use tensor visualization techniques to study seismic behavior of concrete pile foundations embedded in soil. We show results and limitations of current and new techniques leading to a discussion of possible further research.

Keywords: visualization, tensor field, soil structure simulation, hyperstreamlines, hyperstreams-surfaces

1. Introduction

Earthquakes have a devastating effect on mankind. They cost lives and destroy buildings, dams, bridges and other valuable civil infrastructure. There exists an enormous interest to limit seismic effects on foundations and structures. Experience has shown that building technology can reduce damage and save lives as well as increase damage and casualties. Since earthquakes are vibrations of the ground, a detailed study of foundation systems is necessary. In this case study, we concentrate on concrete single piles and pile groups grounded in soil. The Center for Geotechnical Modeling (CGM) at UC Davis is using the finite element method to analyze the mechanics of seismic behavior of soil–foundation–structure interaction (SFSI). The stress and strain tensor fields in the concrete piles and in the soil are of major interest as they control the inelastic (non-linear) response of the system. A sad example for the practical relevance of this research is the failure of the Hanshin Expressway Route 3 in Kobe, Japan, in 1995 [5].

2. Soil-Pile Structure Simulation

The SFSI simulations performed at CGM aim at increasing our understanding of the behavior of the pile–soil systems during strong earthquake events. To this end CGM researchers perform direct, time-dependent, 3D elastic–plastic simulations of solid models representing complete SFSI systems. Simulations are performed on a Beowulf parallel computer system. Post–processing of results from the dynamic analysis of large 3D finite element models tend to be cumbersome if advanced visualization tools are not used.

Of particular interest is the visualization of the dynamic behavior of stress and strain tensor fields. The cyclic nature of those tensor fields is mainly responsible for failures associated with earthquake events.

3. Physical and Mathematical Background

We are dealing with steady and time-dependent stress tensor fields in this case study. These are three-dimensional symmetric, second-order tensor fields. For a precise description, we provide a few basic definitions about tensors. We have also added some basic definitions about stress tensors.

3.1 Tensors

We adopt the notations of Borisenko and Tarapov [1] and Delmarcelle and Hesselink [2]. A (covariant) real tensor of second order and dimension d is a linear map

$$T : R^d \times R^d \rightarrow R.$$

A tensor field

$$\mathcal{T} : R^d \supset V \rightarrow \text{Lin}(R^d \times R^d \rightarrow R)$$

defines a tensor for each position of a region in space. We will always have a single, fixed orthonormal coordinate system in three dimensions in our examples, thus we de-

scribe a tensor by a 3×3 -matrix

$$T = \begin{pmatrix} T_{11} & T_{12} & T_{13} \\ T_{21} & T_{22} & T_{23} \\ T_{31} & T_{32} & T_{33} \end{pmatrix}.$$

A tensor field is, in our case, a map

$$\begin{aligned} \mathcal{T} : R^3 &\rightarrow R^{3 \times 3} \\ (x, y, z) &\mapsto \begin{pmatrix} T_{11} & T_{12} & T_{13} \\ T_{21} & T_{22} & T_{23} \\ T_{31} & T_{32} & T_{33} \end{pmatrix}. \end{aligned} \quad (1)$$

Furthermore, we are concerned with symmetric tensor fields, for which we can use the notation

$$\begin{aligned} \mathcal{T} : R^3 &\rightarrow R^{3 \times 3} \\ (x, y, z) &\mapsto \begin{pmatrix} T_{11} & T_{12} & T_{13} \\ T_{12} & T_{22} & T_{23} \\ T_{13} & T_{23} & T_{33} \end{pmatrix}. \end{aligned} \quad (2)$$

It is well known that a symmetric tensor can always be expressed by its eigenvalues and eigenvectors, i.e., for each tensor, there exist three numbers λ_1, λ_2 , and $\lambda_3 \in R$ and three associated orthogonal vectors v_1, v_2 , and v_3 , respectively, such that

$$T v_i = \lambda_i v_i.$$

Since the three eigenvectors span the whole space and the tensor is linear, the tensor can be described completely by its eigenvalues and eigenvectors.

3.2 Stress Tensor Field

In our application, civil engineers are especially interested in the stress inside piles, on their boundaries and in the soil close to piles. Stress can be defined using stress vectors [4]. Let V be a spatial region covered with a material B , and let S be a closed surface in B . For a small surface element ΔS , let N be the outward unit normal vector. If the outer part exerts a force ΔF on the inner part, we call the ratio

$$T = \frac{\Delta F}{\Delta S}$$

a stress vector. (Formally, we define T as the differential limit dF/dS .) For the stress tensor, we consider a small cube whose edges are aligned with the coordinate axes e_1, e_2, e_3 . Let ΔS_1 be the side having e_1 as normal vector. Then, we define T_{11}, T_{21} , and T_{31} as the components of the stress vector on this surface. By considering ΔS_2 and ΔS_3 , we obtain the other components T_{12}, T_{22}, T_{32} and T_{13}, T_{23}, T_{33} of the stress tensor. The construction is illustrated in Fig. 1 and Fig. 2.

4. Stress and Strain Tensor Visualization

Tensor fields have not yet attracted much attention in the visualization community despite their importance in engineering problems. We have applied some known and some extended techniques to our simulated data and discuss the results in the following.

4.1 Hedgehogs

Our first visualization method is a typical *hedgehog* method. Considering the various known tensor hedgehogs, we use the *tripod*, since it works for positive and negative eigenvalues (unlike ellipsoids). The tripod consists of three orthogonal line segments that indicate the directions of the eigenvectors of the tensor at a single position. Engineers are particularly interested in the tension forces inside a pile. The danger of tension forces results from the fact that concrete can withstand large compression forces but can break under comparably moderate tension forces. Steel re-inforcements are necessary to compensate for the weakness of concrete under tension. Another reason is that engineers are particularly interested in visualizing directions and magnitudes of tensile stresses and compressive stresses. The tripods allow for coloring of eigenvectors by using sign convention. A logical color coding is therefore to color positive eigenvalues (tension) red and negative eigenvalues (compression) green. The length of the line segments indicates the absolute value of the eigenvalue. (Engineers, when first shown this type of representation, required some training to understand the images. Training was done by using simple, well understood examples to illustrate our method.)

For simple illustration purposes, we have used the analytical solution for an infinite half-space with a single point load at the origin, known as *Boussinesq problem*. (It has been used earlier by Hesselink, Levy, and Lavin [6].) We show the result of the hedgehog presentation in Fig. 3. The dominant compression is easily noticed due to the long green line segments. The tensions in the other two directions can also be deduced from the short red line segments. We have applied the tripod hedgehogs to two non-trivial data sets. The result in an one-pile scenario is shown in Fig. 4. One can clearly see the strong forces around the pile cap and the very weak forces below. It is also apparent that this phenomenon is complicated, since the hedgehogs vary heavily. The results with the four-pile cap were similar. In all images, engineers quickly became aware of the classical problem of any hedgehog presentation: There is no way to visually interpolate the data except for simple well understood examples like our analytic data set shown in Fig. 3.

4.2 Hyperstreamlines

Dickinson introduced the concept of *tensor lines* into visualization [3]. These are curves that are everywhere tangent to the major, medium and minor eigenvectors. Their calculation is similar to the numerical calculation of streamlines in vector fields by just using the eigenvectors instead of the vectors. Delmarcelle et al. extended this idea to *hyperstreamlines* [2]. A hyperstreamline is a tensor line with a tube or helix structure defined by the other two eigenvalues and eigenvectors. Dickinson and Delmarcelle describe the algorithms for tensor lines and hyperstreamlines in de-

tail, so the reader may consult the references for further details. Fig. 5 shows some minor hyperstreamlines in a two-point-load scenario. Minor hyperstreamlines in a push-pull scenario are shown in Fig. 6. Some minor tensor lines of the one-pile data set are shown in Fig. 7. Their calculation does not lead to rapid changes, so the numerical calculation can be done without using large stepsize adaptation. The minor hyperstreamlines shown in Fig. 8 already exhibit some problems as a result of large changes of the other two eigenvectors. This is even more evident in the behavior of the major hyperstreamlines shown in Fig. 9. In this example, we stopped the major hyperstreamlines when the major eigenvalue, i.e., all eigenvalues, became negative — since tension is the main problem for concrete. Nevertheless, it can be seen that the forces are difficult to interpret. Fig. 10 exhibits the same problems in the four-pile-group data. Major hyperstreamlines showed a rather chaotic behavior, so we picked the minor hyperstreamlines which show the major eigenvector as one of the diameters.

4.3 Hypersurfaces

For our application, the objective is to obtain a better understanding of the behavior of several tensor lines. Therefore, we investigated the behavior of families of tensor lines. Using sets of open (or closed) curves as starting curves leads to *hypersurfaces*. We have tested this idea for the one point load data set. A minor hypersurface is shown in Fig. 11. A medium hypersurface can be seen in Fig. 12. Fig. 13 shows some of these surfaces on the one-pile data set. The four-pile-group case is given in Fig. 14. The behavior of the tensor lines can be depicted clearly in these examples. We used the simplest method to draw the hyperstreams-surfaces: A user defines a number of uniformly spaced sample points on the curves. The sample points serve as starting points for hyperstreamlines that are propagated in the usual way. The resulting points on the curves are triangulated creating triangle strips between two neighboring curves. A more sophisticated algorithm could be based, for example, on the ideas of Hultquist for stream surface calculations [7]. This leads to the insertion of new intermediate traces if neighboring traces diverge above a threshold for the distance. On the other side, one would remove traces if the two neighboring traces in the list come quite close.

5. Tensor Field Structure

A major goal of our research was the use of structural analysis methods, like topology analysis, for stress and strain tensor field analysis, inside and outside a pile. Any structural analysis has to study carefully the questions of the underlying phenomenon to be useful. In our case, the interest lies on the tension forces. One structural element are the regions with an equal number of positive eigenvalues. Since the tensor values are interpolated continuously over the domain and eigenvalues depend continuously on

the tensors, a change of the number of positive eigenvalues forces a zero eigenvalue in between. This leads to a zero determinant, which happens along surfaces in the general case. Instead of calculating these surfaces exactly, it is possible to simply count the number of positive eigenvalues at each grid point and apply a marching-tetrahedra algorithm with the values 0.5, 1.5, and 2.5 to approximate volumes with zero, one, two, and three positive eigenvalues. The results for the one-pile data set are shown in Fig. 15 and 16. Since there are no points with three positive eigenvalues, we show only the isosurfaces with values 0.5 and 1.5. The civil engineers like these images as there is a direct relation between the number of positive eigenvalues and the kind of breaks in the concrete when the magnitude of the tension is above the “allowable” limit for the concrete.

We are currently working on extending tensor field topology [6], but the degenerate points alone do not provide enough information. More research remains to be done.

6. Conclusions

We have presented an important application for tensor field visualization. Not many techniques exist for tensor field data sets, so we have applied some of them: tripods, tensor lines and hyperstreamlines. Tripods provide some information about the data but fail to preserve the continuous nature of tensor fields that is typical for our driving engineering applications. Tensor lines and hyperstreamlines consider this continuous behavior, but engineers need to apply these methods first to simple, well known examples to get used to them. Hyperstreams-surfaces are a natural extension of tensor lines, since they can be understood as continuous families of tensor lines. Visualizing results from complex 3D simulations will require further study, but even our simple approach works well in some cases.

For our application, a structural analysis can be started by analyzing tension and by extracting surfaces of zero determinant. There is a direct relation between the kinds of cracks in concrete due to large tension forces. A topological analysis of the stress tensor fields will require more research.

7. Acknowledgement

This work was supported by the National Science Foundation under contracts ACI 9624034 and ACI 9983641 (CAREER Awards), through the Large Scientific and Software Data Set Visualization (LSSDSV) program under contract ACI 9982251, and through the National Partnership for Advanced Computational Infrastructure (NPACI); the Office of Naval Research under contract N00014-97-1-0222; the Army Research Office under contract ARO 36598-MA-RIP; the NASA Ames Research Center through an NRA award under contract NAG2-1216; the Lawrence Livermore National Laboratory under ASCI ASAP Level-2 Memorandum Agreement B347878 and under Memorandum Agreement B503159; and the North Atlantic Treaty Organization (NATO) under contract CRG.971628

awarded to the University of California, Davis. We also acknowledge the support of ALSTOM Schilling Robotics and Silicon Graphics. We thank the members of the Visualization Group at the Center for Image Processing and Integrated Computing (CIPIC) at the University of California, Davis. Further, we thank all members of the Computer Graphics Group at the University of Kaiserslautern, especially Tom Bobach, Christoph Garth, Aragorn Rockstroh, Xavier Tricoche, Thomas Wischgoll and Wang Yi for their programming efforts and valuable discussions.

References

- [1] A. I. BORISENKO AND I. E. TARAPOV, *Vector and Tensor Analysis with Applications*, Dover Publications, New York, 1968.
- [2] T. DELMARCELLE AND L. HESSELINK, *Visualizing Second-Order Tensor Fields with Hyperstreamlines*, IEEE Computer Graphics & Applications **13**:4 (1993), pp. 25 – 33.
- [3] R. R. DICKENSON, *A Unified Approach to the Design of Visualization Software for the Analysis of Field Problems*, SPIE Proceedings, Vol. 1083, 1989, pp. 173 – 180.
- [4] Y. C. FUNG, *A First Course in Continuum Mechanics*, Prentice Hall, Englewood Cliffs, NJ, 1998.
- [5] G. GAZETAS AND G. MYLONAKIS, *Seismic Soil-Structure Interaction: New Evidenz and Emerging Issues*, Geotechnical Earthquake Engineering and Soil Dynamics III, 1997, pp. 1119 – 1174.
- [6] L. HESSELINK, Y. LEVY, AND Y. LAVIN, *The Topology of Symmetric, Second-Order 3D Tensor Fields*, IEEE Transactions on Visualization and Computer Graphics **3**:1 (1997), pp. 1 – 11.
- [7] J. P. M. HULTQUIST, *Constructing Stream Surfaces in Steady 3D Vector Fields*, IEEE Visualization '92 (A. E. KAUFMAN AND G. M. NIELSON, eds.), Boston, 1992, pp. 171 – 178.

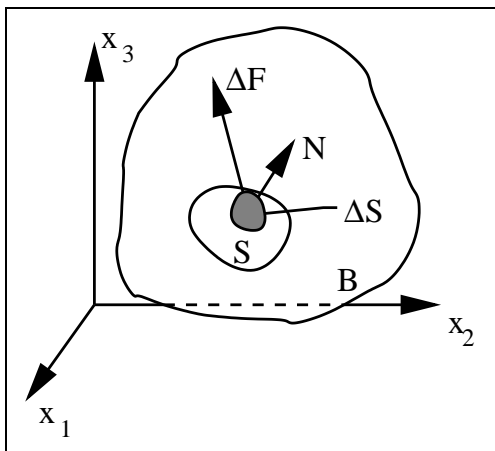


Figure 1. Definition of stress vector.

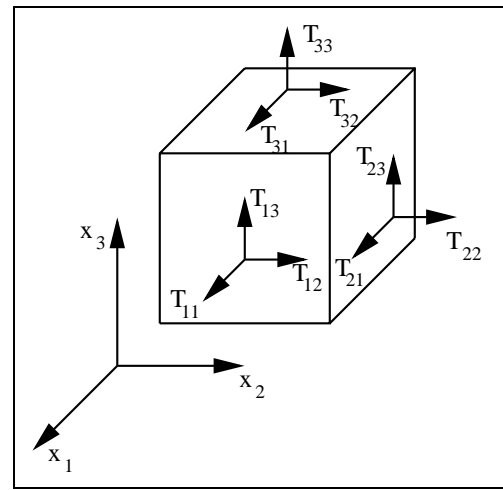


Figure 2. Definition of stress tensor.

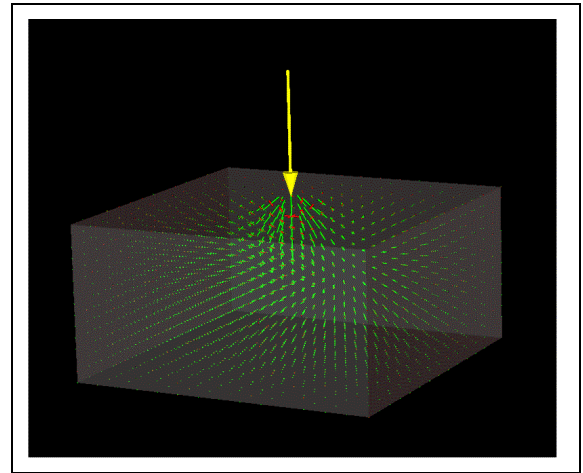


Figure 3. Tripod hedgehogs for single-point-load set.

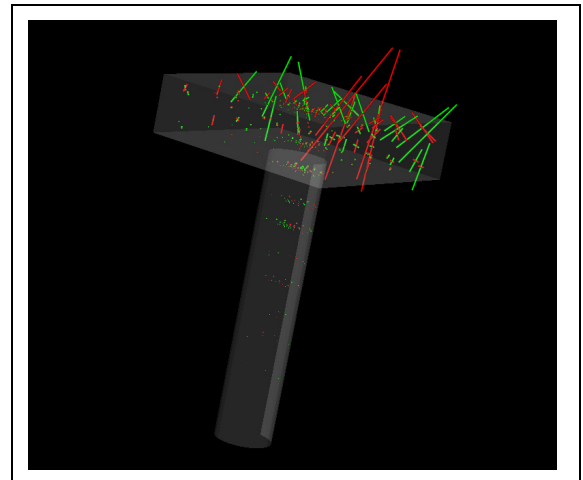


Figure 4. Tripod hedgehogs for one-pile data set.

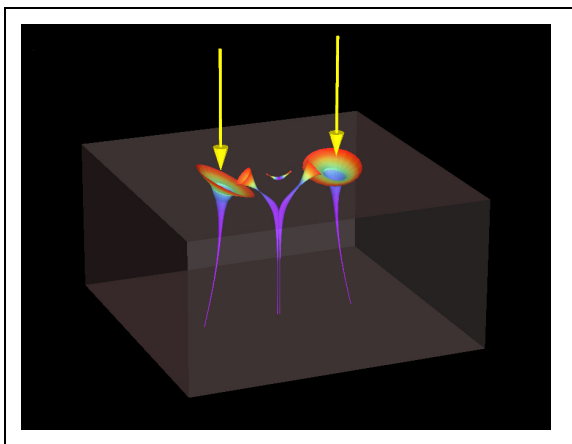


Figure 5. Minor hyperstreamlines for two-point-load data set.

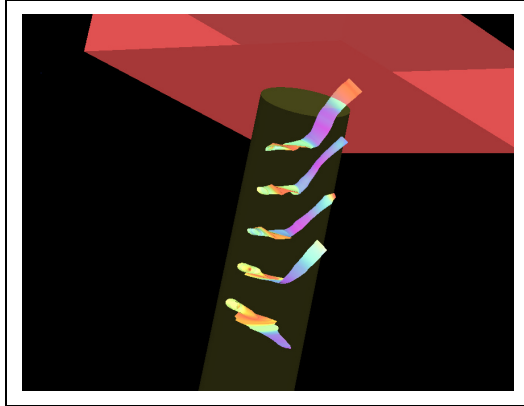


Figure 8. Minor hyperstreamlines for one-pile data set. Varying diameter illustrates rapid changes in other two eigenvalues.

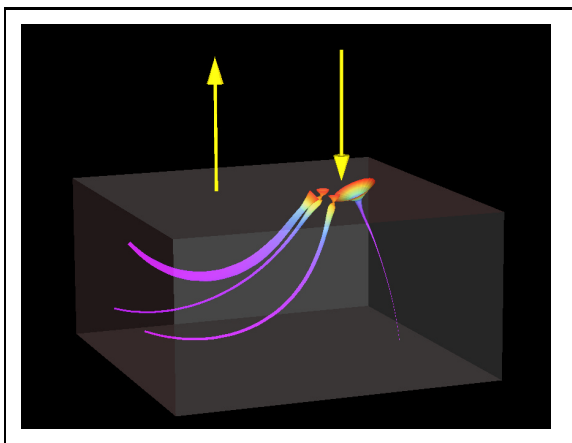


Figure 6. Minor hyperstreamlines for push-pull data set.

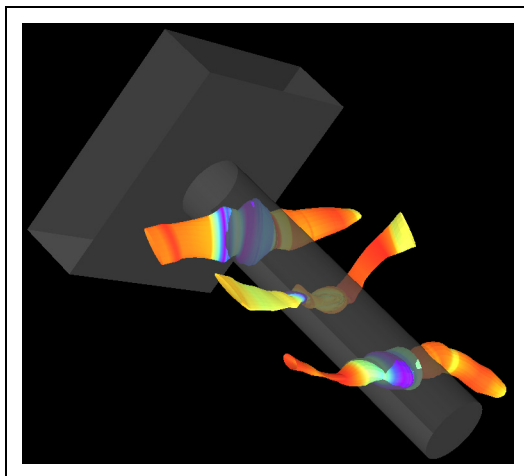


Figure 9. Major hyperstreamlines for one-pile data set.

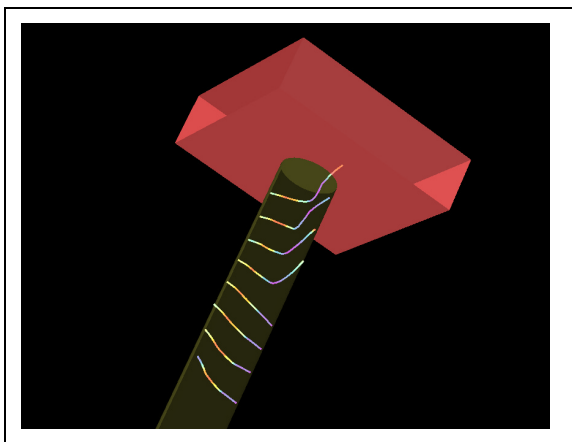


Figure 7. Minor tensor lines inside the concrete of one-pile data set.

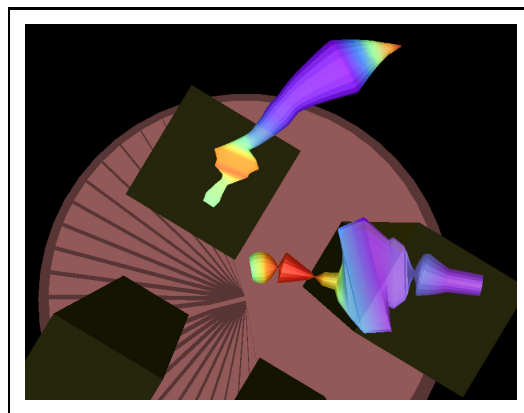


Figure 10. Minor hyperstreamlines for four-pile group data set. Varying diameter indicates problems with other two eigenvector fields.

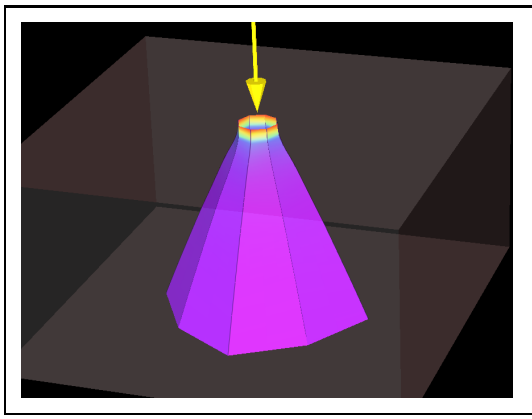


Figure 11. Minor hyperstreamsurfaces for one-point-load data set. The simple “structure” of this tensor data set prevents instability problems in the numerical calculations.

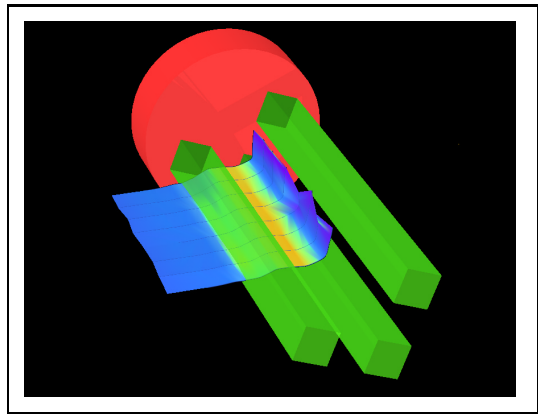


Figure 14. Minor hyperstreamsurface visualizing behavior of a family of minor tensor lines for four-pile-group data set. (We have removed one of the piles to simplify the view.)

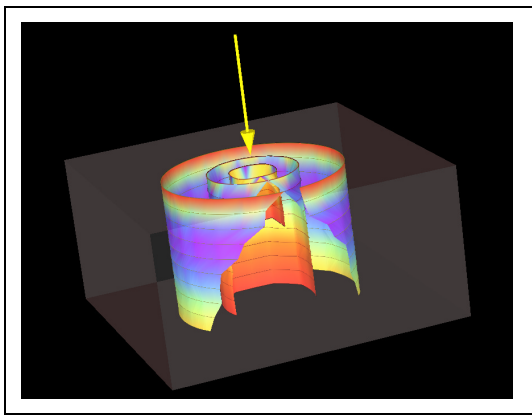


Figure 12. Medium hyperstreamsurfaces for one-point-load data set.

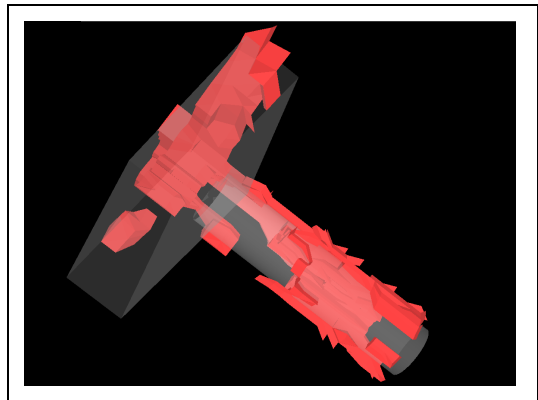


Figure 15. Isosurface of regions with at least one positive eigenvalue of the one-pile data set. (The isosurfaces are limited to the pile and the cells in the soil adjacent to the pile.)

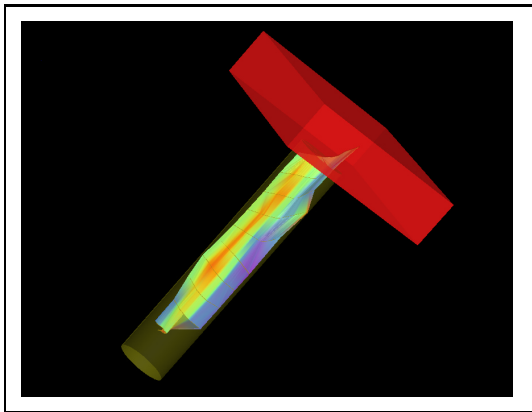


Figure 13. Minor hyperstreamsurface limited to concrete pile. Behavior of a family of minor tensor lines starting at center line of pile becomes evident.

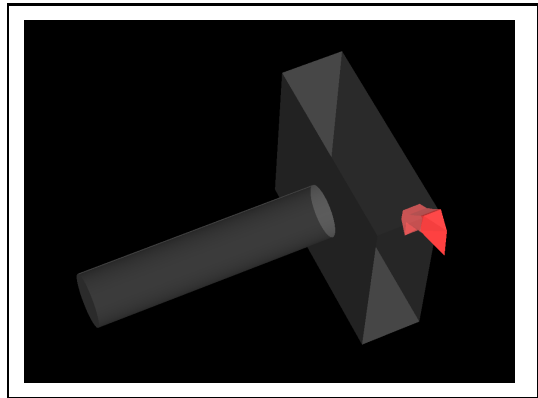


Figure 16. Isosurfaces of regions with at least two positive eigenvalues of the one-pile data set. (The isosurfaces are limited to the pile and the cells in the soil adjacent to the pile.)